

# A Metallocryptand-Based Manganese(II)–Cobalt(II) Ferrimagnet with a Three-Dimensional Honeycomb Open-Framework Architecture\*\*

Departamento de Física Aplicada  
Universidad Politécnica de València  
València 46071 (Spain)

Dr. R. Ruiz-García  
Departament de Química Orgànica  
Institut de Ciència Molecular (ICMOL), and  
Fundació General de la Universitat de València (FGUV)  
Universitat de València  
Paterna 46980, València (Spain)

Dr. J. Cano  
Departament de Química Inorgànica  
Institut de Química Teòrica i Computacional (IQTC) and  
Institut de Nanociència i Nanotecnologia (IN2UB), and  
Institució Catalana de Recerca i Estudis Avançats (ICREA)  
Universitat de Barcelona  
Barcelona 08028 (Spain)

Prof. Dr. P. Amorós  
Institut de Ciència dels Materials (ICMUV)  
Universitat de València  
Paterna 46980, València (Spain)

[\*\*] This work was supported by the Ministerio de Educación y Ciencia (MEC, Spain; projects CTQ2007-61690 and the Consolider-Ingenio in Molecular Science CSD2007-00010), the Ministère de l'Enseignement Supérieur et de la Recherche (MESR, France), the Coordenação de Aperfeiçoamento de Pessoal de Nível Superior (CAPES, Brazil; project COFECUB 460/04), and the Fundação de Amparo à Pesquisa do Estado de Minas Gerais (FAPEMIG, Brazil; projects CEX1837/06 and PRONEX 526/07). D.C., E.P., and M.C.D. thank the CAPES, the MEC, and the MESR/UPMC for grants. J.C. acknowledges the Universitat de València for an invited researcher grant. We are especially indebted to Dr. J.-M. Martínez and Dr. J. El Haskouri for thermogravimetric and gas sorption measurements, respectively.



Supporting information for this article is available on the WWW under <http://www.angewandte.org> or from the author.

*Emilio Pardo, Danielle Cangussu, Marie-Claire Dul, Rodrigue Lescouëzec, Patrick Herson, Yves Journaux,\* Emerson F. Pedroso, Cynthia L. M. Pereira, M. Carmen Muñoz, Rafael Ruiz-García, Joan Cano, Pedro Amorós, Miguel Julve, and Francesc Lloret\**

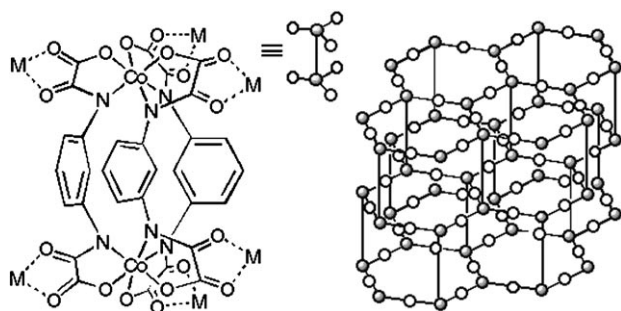
The design and synthesis of simple molecules containing paramagnetic metal centers that are able to self-assemble through metal–ligand interactions into supramolecular assemblies of increasing structural and magnetic complexity is a major challenge in modern (supra)molecular coordination chemistry and (supra)molecular magnetism.<sup>[1–4]</sup> Discrete zero-dimensional polynuclear coordination compounds as well as infinite one-, two-, or three-dimensional coordination polymers, also known as metal–organic frameworks (MOFs),<sup>[5]</sup> are included in this category. The overall structure and magnetic properties of the final *n*D products (*n* = 0–3) rely on the judicious choice of the metal building block, especially the substitution pattern and steric requirements of the bridging ligand and the electronic configuration and magnetic anisotropy of the metal ion. Such multidimensional

[\*] Dr. E. Pardo, Dr. D. Cangussu, M. C. Dul, Dr. R. Lescouëzec, P. Herson, Dr. Y. Journaux  
Laboratoire de Chimie Inorganique et Matériaux Moléculaires  
Université Pierre et Marie Curie-Paris 6, UMR 7071  
Paris 75252 (France)  
Fax: (+33) 144-273-841  
E-mail: jour@ccr.jussieu.fr

Prof. Dr. M. Julve, Prof. Dr. F. Lloret  
Departament de Química Inorgànica  
Institut de Ciència Molecular (ICMOL)  
Universitat de València  
Paterna 46980, València (Spain)  
Fax: (+34) 963-544-859  
E-mail: francisco.lloret@uv.es

Dr. E. F. Pedroso  
Departamento de Química  
Centro Federal de Educação Tecnológica de Minas Gerais  
Belo Horizonte-MG 30480-000, Minas Gerais (Brazil)

Dr. C. L. M. Pereira  
Departamento de Química  
Universidade Federal de Juiz de Fora  
Juiz de Fora 36036-330, Minas Gerais (Brazil)  
Prof. Dr. M. C. Muñoz



**Scheme 1.** The proposed 3D honeycomb open-framework resulting from the metal-mediated self-assembly of the hexakis(bidentate) dicobalt(II) complex  $[\text{Co}_2(\text{mpba})_3]^{8-}$  with  $\text{M}^{n+}$  ions ( $\text{M}^{n+} = \text{Li}^+$  or  $\text{Mn}^{2+}$ ).

species are of great importance in the so-called “bottom-up” approach to molecular magnetic materials, particularly the low-dimensional single-molecule (SMMs) or single-chain (SCMs) magnets and the higher-dimensionality molecule-based magnets, all of which have potential applications in information storage and processing nanotechnology.<sup>[6–8]</sup>

Our strategy in this field is based on combining mono-, di-, and trinuclear late 3d transition metal complexes with a novel family of aromatic polyoxamato ligands as building blocks for the rational design of oxamato-bridged high-nuclearity coordination compounds and high-dimensionality coordination polymers with interesting magnetic properties.<sup>[9–12]</sup> In particular, the triple-stranded dinuclear cobalt(II) complex  $[\text{Co}_2(\text{mpba})_3]^{8-}$  [mpba = 1,3-phenylenebis(oxamato)] enables the formation of double-propeller octanuclear coordination compounds with a metallacryptand core when acting as a hexakis(bidentate) ligand (Scheme 1, left). Such coordination compounds could constitute the basic structural unit for the construction of 3D open-frameworks with a “honeycomb” architecture and a (6,4) net topology (Scheme 1, right). Herein we report the synthesis, crystal structures, and magnetic properties of the oxamato-bridged heterobimetallic 3D compounds  $\text{Li}_3[\text{Li}_3\text{Co}_2(\text{mpba})_3(\text{H}_2\text{O})_6] \cdot 31 \text{H}_2\text{O}$  (**1**) and  $\text{Li}_2[\text{Mn}_3\text{Co}_2(\text{mpba})_3(\text{H}_2\text{O})_6] \cdot 22 \text{H}_2\text{O}$  (**2**). A preliminary study of their sorption ability toward solvent molecules and gases is also provided.

Compounds **1** and **2** were prepared by the metal-mediated self-assembly of the corresponding octaanionic dicobalt(II) precursor  $[\text{Co}_2(\text{mpba})_3]^{8-}$  with univalent lithium(I) or divalent manganese(II) ions, respectively, in water (see *Experimental Section*). The polymerization reaction with  $\text{Li}^+$  ions allows for a slow crystallization process upon diffusion of methanol vapor into an aqueous solution, which provides single crystals of low quality but good enough for a complete X-ray structure determination. Interestingly, crystals of **1** slowly decompose when separated from the mother liquor in the open air, although their crystallinity is recovered in contact with methanol. In contrast, the polymerization reaction with  $\text{Mn}^{II}$  ions in water is too fast to give a crystalline material (even when using common slow diffusion techniques in an H-shaped tube). Once filtered, the initial gelatinous precipitate of **2** evolves into a powdered solid after several hours in air, most likely because of partial loss of the adsorbed

water molecules. Compound **2** is, in fact, amorphous, as revealed by its X-ray powder diffraction pattern, which shows no well-resolved peaks. Its elemental analysis nevertheless confirms the expected 3:2 Mn:Co molar ratio.

The thermogravimetric analyses of **1** and **2** in the temperature range 25–300 °C under dry air atmosphere show a qualitatively similar behavior, in agreement with their open-framework nature (see Figure S1 in the Supporting Informa-

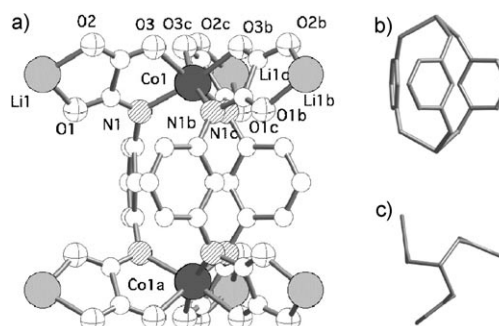


**Figure 1.** a) Perspective view of the asymmetric unit of **1** showing the atom labeling for the metal coordination environment (coordinated water molecules and hydrogen atoms have been omitted for clarity). Symmetry codes: a:  $x, y, 1/2 - z$ ; b:  $-\gamma, x - \gamma, z$ ; c:  $\gamma - z, -x, z$ . b) Side and c) top projections of the *meso*-helicate-type metallacryptand core.

tion). In general, the fast weight loss that occurs from room temperature to around 120 °C is followed by a gradual weight loss upon further heating to 300 °C. The values of the mass loss percentage below 120 °C are 30 % for **1** and 20 % for **2** (corresponding to twenty five and sixteen water molecules per  $\text{M}_3\text{Co}_2$  unit, respectively). This mass loss is attributed to partial liberation of the weakly bound crystallization water molecules.

The  $\text{N}_2$  adsorption isotherms for **1** and **2** were recorded at 77 K after complete evacuation at 70 and 120 °C. Irrespective of the conditions, almost no porosity relative to  $\text{N}_2$  was observed for **1** and **2** (BET surface areas of 3 and 5  $\text{m}^2 \text{g}^{-1}$ , respectively), possibly due to an efficient blocking of the pores by the lithium counteranions, which prevents the achievement of any permanent porosity. Nevertheless, a certain degree of pore accessibility is suggested under mild conditions in liquid media by the qualitative reactivity of **1** toward methanol.

The structure of **1** consists of triple-stranded  $[\text{Co}^{II}_2(\text{mpba})_3]^{8-}$  anions, with  $C_{3h}$  molecular symmetry, coordinated and noncoordinated lithium(I) cations, and coordinated and crystallization water molecules (Figure 1). The symmetrically related atoms Co1 and Co1a exhibit a trigonally distorted octahedral  $\text{CoN}_3\text{O}_3$  coordination environment [trigonal twist angle of 47.8(3)°] containing three amidate-nitrogen and three carboxylate-oxygen atoms from the oxamato groups of the three bis(bidentate) dinucleating ligands (Figure 1 a). The Co1–N1 and Co1–O3 distances [2.106(8) and 2.137(8) Å, respectively] are typical of high-spin  $\text{Co}^{II}$  ions. The two octahedral metal-tris(oxamate) moieties of opposite chirality ( $\Delta\Lambda$  form) are connected by three *m*-phenylene spacers, which leads to a metallacryptand core of the *meso*-helicate type (Figures 1 b and c). The aromatic groups within this

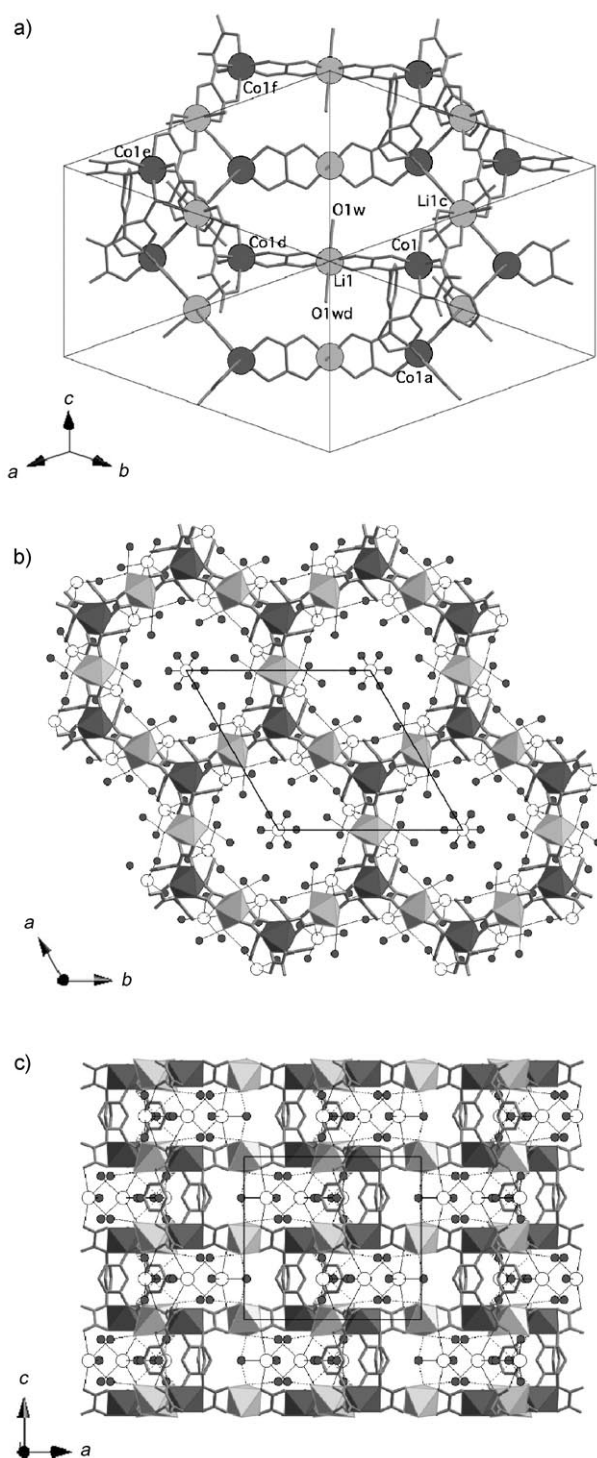


**Figure 2.** a) Perspective view of a hexagonal prismatic cell of **1** showing the atom labeling for the metal atoms [symmetry codes: a:  $x, y, 1/2 - z$ ; c:  $y - z, -x, z$ ; d:  $-x, -y, -z$ ; e:  $x, y - 1, z$ ; f:  $1 - x, 1 - y, -z$ ]. b) and c) Projection views of the honeycomb three-dimensional framework along the  $c$  and  $b$  axes, respectively (weak interactions with the lithium counteranions and hydrogen bonds with the water molecules are represented by solid and dotted lines, respectively).

dinuclear  $\text{Co}_2(m\text{-N}_2\text{C}_6\text{H}_4)_3$  metallacryptand core are disposed edge-to-face, with a weak  $\text{C-H}\cdots\pi$  interaction between

neighboring benzene rings. The average torsion angle ( $\alpha$ ) around the  $\text{Co1-N1-C1-C2}$  bonds is  $94.0(9)^\circ$ .

The binding of these heterochiral *meso*-helicite-type  $\text{Co}^{\text{II}}_2$  metallacryptands to axially distorted octahedral *trans*-diaqualithium(I) ions through the two *cis* carbonyl-oxygen atoms of the oxamato groups [ $\text{Li1-O1} = 1.962(9)$ ,  $\text{Li(1)-O(2)} = 2.039(11)$ , and  $\text{Li(1)-O(1w)} = 2.65(2)$  Å] leads to the expected 3D honeycomb framework (Figure 2). Such outward coordination has rarely been exploited for metallacryptands (helicates and *meso*-helicates), although inward coordination to give metallacryptates is commonly observed.<sup>[13]</sup> The basic hexagonal prismatic unit cell in **1** consists of twelve and ten metal sites per hexagonal and rectangular face, respectively: six Co1 atoms of opposite propeller chirality ( $\Delta$  and  $\Lambda$ ) alternate regularly at the corners of each hexagon or at the four corners and the mid-point of the two long edges of each rectangle, whereas either six or four Li1 atoms sit at the middle of each edge of the hexagon or at the one-quarter and three-quarter point of each long edge of the rectangle, respectively (Figure 2a).

The 3D honeycomb framework of **1** can alternatively be described as an infinite parallel array of anionic oxamato-bridged  $\text{Li}_3\text{Co}^{\text{II}}_2$  hexagonal layers growing in the  $ab$  plane (Figure 2b) where the adjacent layers are interconnected through three *m*-phenylenediamide bridges between the  $\text{Co}^{\text{II}}$  ions of opposite propeller chirality ( $\Delta$  and  $\Lambda$ ) to give dinuclear metallacryptand cores of the *meso*-helicite type which act as pillars of the hexagonal prismatic lattice (Figure 2c). The intralayer  $\text{Li1-Co1}$  distance through the oxamato bridge is  $5.396(5)$  Å, while the interlayer  $\text{Co1-Co1a}$  distance through the triple *m*-phenylenediamide bridge is  $6.851(3)$  Å. Overall, this leads to an open-framework structure with small hexagonal pores along the  $c$  axis of  $21.547(3)$  Å in diameter (defined as the  $\text{Co1-Co1f}$  distance between directly opposed metal atoms in the hexagon), which are occupied by hydrogen-bonded crystallization water molecules and  $[\text{Li}(\text{H}_2\text{O})_6]^+$  counteranions. Hence, the solvated Li2 atoms are weakly bound to the surface of the metallo-organic framework through the carbonyl-oxygen atoms from the oxamato groups [ $\text{Li2-O2} = 3.07(3)$ ,  $\text{Li2-O2w} = 2.99(7)$ ,  $\text{Li2-O3w} = 3.00(6)$ ,  $\text{Li2-O4w} = 2.23(7)$ , and  $\text{Li2-O6w} = 3.07(8)$  Å; Figure 2c], whereas linear arrays of fully solvated Li3 and Li4 atoms bridged by three water molecules [ $\text{Li3-O5w} = 2.72(5)$  and  $\text{Li4-O5w} = 2.12(7)$  Å] are hosted in the central cavity of the pores (Figure 2b). The calculated volume accessible by a small molecule (like  $\text{H}_2\text{O}$ ) is  $884$  Å<sup>3</sup>, which represents less than 20% of the potential void per unit cell volume ( $4474$  Å<sup>3</sup>; see Figure S2 in the Supporting Information).

Compounds **1** and **2** show a distinct magnetic behavior depending on the diamagnetic or paramagnetic nature of the coordinated uni- or divalent octahedral M ion ( $\text{M} = \text{Li}^{\text{I}}$  or  $\text{Mn}^{\text{II}}$ , respectively). The  $\chi_{\text{M}}T$  vs.  $T$  plot ( $\chi_{\text{M}}$  is the molar magnetic susceptibility per  $\text{Li}_3\text{Co}_2$  unit) of **1** is characteristic of rather well-isolated, weakly ferromagnetically coupled dicobalt(II) pairs (Figure 3a). Upon cooling,  $\chi_{\text{M}}T$  decreases from  $5.73$  cm<sup>3</sup>mol<sup>-1</sup>K at room temperature to reach a minimum of  $3.62$  cm<sup>3</sup>mol<sup>-1</sup>K at  $12.0$  K and then increases up to  $4.09$  cm<sup>3</sup>mol<sup>-1</sup>K at  $2.0$  K. This final increase of  $\chi_{\text{M}}T$  in

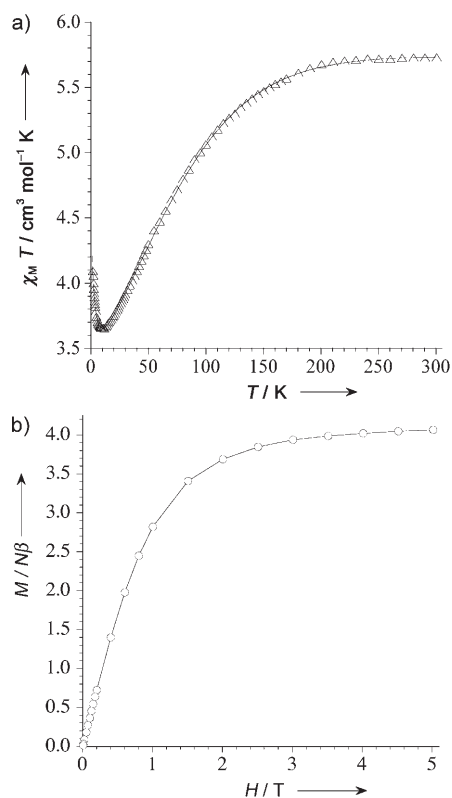


**Figure 3.** a) Temperature dependence of  $\chi_M T$  ( $\Delta$ ) for **1** (the solid line is the best-fit curve). b) Field dependence of  $M$  ( $\circ$ ) for **1** at 2.0 K (the solid line is a guide for the eye and has no other significance).

the low-temperature region is indicative of a moderately weak ferromagnetic coupling between the two high-spin  $\text{Co}^{\text{II}}$  ions, while the decrease of  $\chi_M T$  in the high-temperature region can be attributed to spin–orbit coupling. In general, six-coordinate  $\text{Co}^{\text{II}}$  ions present an important first-order orbital momentum, which means that the spin-Hamiltonian is insufficient to treat the magnetic properties of the cobalt(II) complexes and must be supplemented by considering the orbitally dependent exchange interactions as well as spin–orbit coupling effects.<sup>[14]</sup> We have recently shown that the magnetic properties of six-coordinate dinuclear cobalt(II) complexes can be appropriately described by using a Hamiltonian which includes four terms [Eq. (1)]: a) the magnetic

$$\hat{H} = -J\hat{S}_1\hat{S}_2 - \sum_{i=1}^2 \alpha\lambda\hat{L}_i\hat{S}_i + \sum_{i=1}^2 \Delta[\hat{L}_{zi}^2 - 2/3] + \beta H \sum_{i=1}^2 (-\alpha\hat{L}_i + g_e\hat{S}_i)(1)$$

exchange coupling between the two spin quartets ( $S_1 = S_2 = 3/2$ ) of the  $\text{Co}^{\text{II}}$  ions, b) the spin–orbit coupling of the  $^4\text{T}_1$  ground term in octahedral symmetry, c) the splitting of the  $\text{T}_1$  orbital term into a singlet and a doublet orbital term ( $\Delta$  being the energy gap) due to an axial symmetry, and d) the Zeeman interaction<sup>[15]</sup> where  $\lambda$  is the spin–orbit coupling parameter and  $\alpha$  is an orbital reduction factor defined as  $\alpha = Ak$ . The parameter  $k$  takes into account the reduction of the orbital momentum caused by the delocalization of the unpaired electrons and  $A$  is a crystal field parameter ( $A = 1.5$  and  $1$  for

the weak and strong crystal-field limits, respectively). In the event of isomorphism of the terms  $\text{T}_1$  and  $\text{P}$ , in other words  $L(\text{T}_{1g}) = -AL(\text{P})$ , we can consider  $L$  to be  $1$  and we can treat the term  $\alpha\lambda\hat{L}\hat{S}$  as an isotropic Hamiltonian describing the interaction between the two angular momenta  $L = 1$  and  $S = 3/2$ , with  $-\alpha\lambda$  being the coupling parameter.

A least-squares fit of the magnetic susceptibility data of **1** gave  $\lambda = -116.3 \text{ cm}^{-1}$ ,  $\alpha = 1.10$  (that is,  $k = 0.79$  with  $A = 1.4$ ),  $\Delta = 108 \text{ cm}^{-1}$ , and  $J = +1.03 \text{ cm}^{-1}$  (solid line in Figure 3a). The calculated  $J$  value for **1** agrees both in sign and magnitude with that found for the dinickel(II) metallacryptand analogue ( $J = +3.6 \text{ cm}^{-1}$ ).<sup>[11b]</sup> The ferromagnetic exchange interaction between the two high-spin  $\text{M}^{\text{II}}$  ions ( $\text{M} = \text{Ni}$  or  $\text{Co}$ ) across the

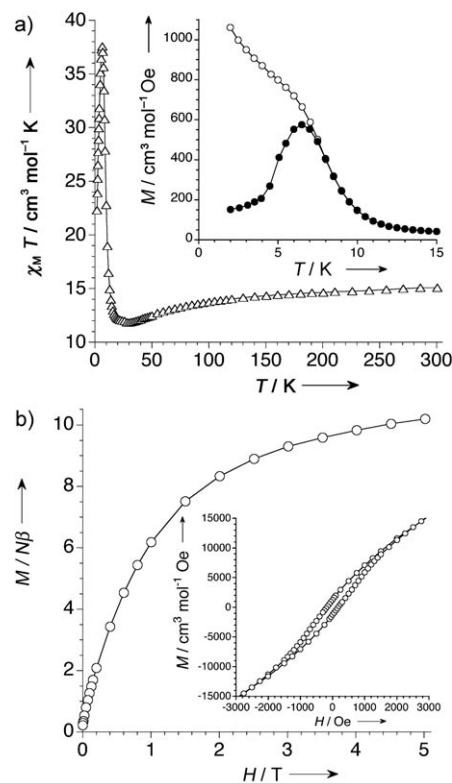


**Figure 4.** a) Temperature dependence of  $\chi_M T$  ( $\Delta$ ) for **2**. The inset shows the FCM ( $\circ$ ) and ZFCM ( $\bullet$ ) curves. b) Field dependence of  $M$  ( $\circ$ ) for **2** at 2.0 K. The inset shows the hysteresis loop (the solid lines are a guide for the eye and have no other significance).

triple *m*-phenylenediamide bridge is due to a spin-polarization mechanism, as observed previously for a related dicopper(II) metallacyclopentane complex ( $J = +16.8 \text{ cm}^{-1}$ ).<sup>[10a]</sup> The next-nearest-neighbor magnetic interactions between the high-spin  $\text{Co}^{\text{II}}$  ions through the coordinated diamagnetic  $\text{Li}^{\text{I}}$  ions are negligible given the large intermolecular metal–metal separation (approx.  $10.8 \text{ \AA}$ ).

The  $M$  vs.  $H$  plot ( $M$  is the molar magnetization per  $\text{Li}_3\text{Co}_2$  unit) for **1** at 2.0 K shows a saturation magnetization of  $4.07 N\beta$  (Figure 3b). This value agrees with that calculated for two  $\text{Co}^{\text{II}}$  ions with an effective  $S'_{\text{Co}} = 1/2$  state and a  $g_{\text{Co}}$  value of  $4.07$  given by  $g_{\text{Co}} = (10 + 2\alpha)/3$  ( $M_s = 2g_{\text{Co}}S'_{\text{Co}}N\beta =$



4.07  $N\beta$ ). Only the ground Kramer's doublet of each  $\text{Co}^{\text{II}}$  ion is populated at 2.0 K.

The magnetic behavior of **2** in the high-temperature region is governed by the moderately strong antiferromagnetic coupling between the high-spin  $\text{Mn}^{\text{II}}$  ( $S_{\text{Mn}} = 5/2$ ) and  $\text{Co}^{\text{II}}$  ( $S_{\text{Co}} = 3/2$ ) ions through the oxamate bridge such that their local spins are aligned in opposite directions (antiparallel) within the plane. This fact results in an overall 2D ferrimagnetic behavior, as evidenced by the characteristic minimum at 30 K in the  $\chi_{\text{M}}T$  vs.  $T$  plot ( $\chi_{\text{M}}$  is the molar magnetic susceptibility per  $\text{Mn}_3\text{Co}_2$  unit) for **2** (Figure 4a). In fact, the value of the saturation magnetization (per  $\text{Mn}_3\text{Co}_2$  unit) of 10.20  $N\beta$  for **2** at 2.0 K is consistent with that predicted for an antiparallel alignment of the spins of  $\text{Mn}^{\text{II}}$  ( $S_{\text{Mn}} = 5/2$ ) and  $\text{Co}^{\text{II}}$  ( $S'_{\text{Co}} = 1/2$ ) ions [ $M_{\text{s}} = (3g_{\text{Mn}}S_{\text{Mn}} - 2g_{\text{Co}}S'_{\text{Co}})N\beta = 10.93 N\beta$  with  $g_{\text{Mn}} = 2.00$  and  $g_{\text{Co}} = 4.07$ ]. Moreover, the magnetization isotherm at 2.0 K does not saturate but shows a relatively large slope at low field values (Figure 4b), thereby revealing a strong short-range correlation within the plane because of the large antiferromagnetic coupling between the high-spin  $\text{Mn}^{\text{II}}$  and  $\text{Co}^{\text{II}}$  ions through the oxamate bridge. An effective ferromagnetic coupling between the oxamato-bridged ferrimagnetic planes is still likely to be operative in the low-temperature region, however, owing to the weak ferromagnetic interaction between the high-spin  $\text{Co}^{\text{II}}$  ions across the *m*-phenylenediamidate bridges within the dinuclear metallacryptand  $\text{Co}^{\text{II}}_2$  linking units, which means that a long-range interplanar magnetic correlation is expected for **2**.

The 3D magnetic ordering in **2** is revealed by the temperature dependence of the field-cooled magnetization (FCM) and the zero-field-cooled magnetization (ZFCM; inset of Figure 4a). The FCM curve, measured by cooling the sample within a very small field of 50 Oe, increases sharply below about 10 K, thereby suggesting the onset of a long-range ferromagnetic transition. The ZFCM curve, measured by cooling the sample in strictly zero field and then warming the sample in the presence of a small field of 50 Oe, shows the expected maximum at  $T_{\text{C}} = 6.5$  K. Indeed, the ferromagnetic nature of the transition is confirmed by the magnetic hysteresis loop at 2.0 K (inset of Figure 4b), which is characteristic of a soft magnet, as evidenced by the moderately low values of the coercive field ( $H_{\text{c}} = 175$  Oe) and the remnant magnetization ( $M_{\text{r}} = 1205 \text{ cm}^3 \text{ mol}^{-1} \text{ Oe}$ ).

In conclusion, we have reported a suitably designed, ferromagnetically coupled, highly anisotropic dicobalt(II) metallacryptand complex containing a *m*-phenylenebis(oxamato) ligand, which self-assembles through either univalent lithium(I) or divalent manganese(II) ions. This metal-mediated self-assembly affords anionic 3D honeycomb open-frameworks of  $\text{M}_3\text{Co}_2$  stoichiometry ( $\text{M} = \text{Li}^{\text{I}}$  or  $\text{Mn}^{\text{II}}$ ) that contain linear arrays of water-bridged lithium(I) ions. The triple *meta*-substituted phenylene linkers in the metallacryptand-based  $\text{Mn}^{\text{II}}_3\text{Co}^{\text{II}}_2$  compound ensure a ferromagnetic interaction between the oxamato-bridged manganese(II)/cobalt(II) ferrimagnetic planes, which leads to a long-range 3D ferromagnetic order at  $T_{\text{C}} = 6.5$  K. The presence of counterbalancing solvated lithium(I) cations as hosts within the pore system of the anionic open-framework structure accounts for its limited sorption capacity toward solvent

molecules and gases. Future work will focus on the preparation of neutral 3D honeycomb open-frameworks with an  $\text{Mn}^{\text{II}}_3\text{M}^{\text{III}}_2$  stoichiometry from novel dinuclear metallacryptand complexes containing trivalent metal ions ( $\text{M} = \text{Fe}$  or  $\text{Cr}$ ) in order to obtain porous magnets.

## Experimental Section

**$\text{Li}_5[\text{Li}_3\text{Co}_2(\text{mpba})_3(\text{H}_2\text{O})_6] \cdot 31 \text{ H}_2\text{O}$  (**1**):** A solution of  $\text{Co}(\text{NO}_3)_2 \cdot 6 \text{ H}_2\text{O}$  (0.58 g, 2.0 mmol) in 15 mL of water was added dropwise, whilst stirring, to an aqueous solution (35 mL) of the diethyl ester derivative of the proligand  $\text{H}_4\text{mpba}$  (0.92 g, 3.0 mmol), which was prepared as reported previously,<sup>[10a]</sup> and  $\text{LiOH} \cdot \text{H}_2\text{O}$  (0.50 g, 12.0 mmol). Large, pink, hexagonal prisms of **1** suitable for X-ray diffraction were obtained from the filtered deep pink solution by slow vapor diffusion of methanol at room temperature. Yield: 1.0 g (63 %); elemental analysis calcd. (%) for  $\text{C}_{30}\text{H}_{86}\text{Co}_2\text{Li}_8\text{N}_6\text{O}_{55}$  (1584): C 22.73, H 5.43, Co 7.44, N 5.30; found: C 23.14, H 5.26, Co 7.30, N 5.39; IR (KBr):  $\tilde{\nu} = 3426$  (O–H),  $1592 \text{ cm}^{-1}$  (C=O).

**$\text{Li}_5[\text{Mn}_3\text{Co}_2(\text{mpba})_3(\text{H}_2\text{O})_6] \cdot 22 \text{ H}_2\text{O}$  (**2**):** A solution of  $\text{Mn}(\text{NO}_3)_2 \cdot 4 \text{ H}_2\text{O}$  (0.38 g, 1.5 mmol) in 15 mL of water was added dropwise to a filtered aqueous solution (35 mL) of the lithium salt of the dicobalt(II) precursor **1** (0.80 g, 0.5 mmol) with continuous stirring at room temperature. The gelatinous precipitate that formed immediately was collected on filter paper and air-dried to give a deep green solid after standing for several hours at room temperature. Yield: 0.6 g (80 %); elemental analysis calcd. (%) for  $\text{C}_{30}\text{H}_{68}\text{Co}_2\text{Li}_2\text{Mn}_3\text{N}_6\text{O}_{46}$  (1545): C 23.30, H 4.40, Co 7.62, Mn 10.66, N 5.44; found: C 23.65, H 4.25, Co 7.55, Mn 10.56, N 5.60; IR (KBr):  $\tilde{\nu} = 3423$  (O–H),  $1596 \text{ cm}^{-1}$  (C=O).

Crystal data for **1**:  $\text{C}_{30}\text{H}_{86}\text{Co}_2\text{Li}_8\text{N}_6\text{O}_{55}$ ,  $M_{\text{r}} = 1584.4$ , hexagonal, space group  $P6_{\text{mm}}$ ,  $a = 18.6580(16)$ ,  $b = 18.6580(16)$ ,  $c = 14.8400(12) \text{ \AA}$ ,  $V = 4474.0(7) \text{ \AA}^3$ ,  $T = 293(2) \text{ K}$ ,  $Z = 4$ ,  $\rho_{\text{calcd}} = 1.176 \text{ g cm}^{-3}$ ,  $\mu(\text{MoK}\alpha) = 0.462 \text{ mm}^{-1}$ ; 2682 unique reflections, 1860 observed with  $I > 2\sigma(I)$ . The structure was solved by direct methods and refined with the full-matrix least-squares technique on  $F^2$  using the programs SHELXS-97 and SHELXL-97. The hydrogen atoms of the organic ligand and the water molecules were neither found nor calculated. One of the four lithium atoms (Li4) was found to be disordered over two positions with an occupancy factor of 0.5 each. Refinement of 77 variables with isotropic thermal parameters for all atoms, except for the cobalt atom, which was refined anisotropically, gave  $R = 0.1811$ ,  $wR = 0.4702$ , and  $GOF = 1.554$  (observed data). The low quality of the resolution likely arises from weak data sets due to the poor crystal quality. In spite of this, the dinuclear anion was clearly defined and its essential structural and crystal-packing features could be reasonably discussed. CCDC-669577 contains the supplementary crystallographic data for this paper. These data can be obtained free of charge from The Cambridge Crystallographic Data Centre via [www.ccdc.cam.ac.uk/data\\_request/cif](http://www.ccdc.cam.ac.uk/data_request/cif).

Thermogravimetric analyses were performed under a static air atmosphere with a Mettler Toledo TGA/STDA 851° thermobalance at a heating rate of  $10 \text{ K min}^{-1}$ .  $\text{N}_2$  adsorption–desorption isotherms at  $-196^\circ\text{C}$  were recorded with a Micromeritics ASAP-2010 automated instrument. Samples were degassed at 70 and  $130^\circ\text{C}$  for 15 h at  $10^{-6}$  Torr prior to analysis. The BET model was used to estimate the surface areas.

Variable-temperature (2.0–300 K) magnetic susceptibility and variable-field (0–5 T) magnetization measurements were carried out with a Quantum Design SQUID magnetometer. The magnetic data were corrected for the diamagnetism of the constituent atoms and for the sample holder.

Received: January 15, 2008

Published online: April 11, 2008

**Keywords:** cobalt · lithium · manganese · materials science · molecular magnets

- [1] M. Pilkington, S. Decurtins in *Comprehensive Coordination Chemistry II: From Biology to Nanotechnology*, Vol. 7 (Eds.: J. A. McCleverty, T. J. Meyer), Elsevier, Oxford, **2004**, p. 177.
- [2] a) M. Verdaguer, A. Bleuzen, V. Marvaud, J. Vaissermann, M. Seuleiman, C. Desplanches, A. Scullier, C. Train, R. Garde, G. Gelly, C. Lomenech, I. Rosenman, P. Veillet, C. Cartier, F. Villain, *Coord. Chem. Rev.* **1999**, 190–192, 1023; b) M. Ohba, H. Okawa, *Coord. Chem. Rev.* **2000**, 198, 313; c) L. M. C. Beltran, J. R. Long, *Acc. Chem. Res.* **2005**, 38, 325; d) R. Lescouëzec, L. M. Toma, J. Vaissermann, M. Verdaguer, F. S. Delgado, C. Ruiz-Pérez, F. Lloret, M. Julve, *Coord. Chem. Rev.* **2005**, 249, 2691.
- [3] a) S. Decurtins, R. Pellaux, G. Antorrena, F. Palacio, *Coord. Chem. Rev.* **1999**, 190–192, 841; b) E. Coronado, M. Clemente-León, J. R. Galán-Mascarós, C. Giménez-Saiz, C. J. Gómez-García, E. Martínez-Ferrero, *J. Chem. Soc. Dalton Trans.* **2000**, 3955; c) M. Gruselle, C. Train, K. Boubekeur, P. Gredin, N. Ovanesyan, *Coord. Chem. Rev.* **2006**, 250, 2491.
- [4] a) O. Kahn, *Struct. Bonding* **1987**, 68, 89; b) O. Kahn, *Acc. Chem. Res.* **2000**, 33, 647; c) R. Ruiz, J. Faus, F. Lloret, M. Julve, Y. Journaux, *Coord. Chem. Rev.* **1999**, 193–195, 1069.
- [5] a) S. R. Batten, R. Robson, *Angew. Chem.* **1998**, 110, 1558; *Angew. Chem. Int. Ed.* **1998**, 37, 1460; b) C. Janiak, *Dalton Trans.* **2003**, 2781; c) D. Maspoch, D. Ruiz-Molina, J. Veciana, *Chem. Soc. Rev.* **2007**, 36, 770; d) G. Férey, *Chem. Soc. Rev.* **2008**, 37, 191.
- [6] a) D. Gatteschi, R. Sessoli, J. Villain, *Molecular Nanomagnets*, Oxford University Press, Oxford, **2006**; b) D. Gatteschi, R. Sessoli, *Angew. Chem.* **2003**, 115, 278; *Angew. Chem. Int. Ed.* **2003**, 42, 268.
- [7] a) C. Coulon, H. Miyasaka, R. Clérac, *Struct. Bonding* **2006**, 122, 163; b) H. Miyasaka, M. Yamashita, *Dalton Trans.* **2007**, 399.
- [8] a) O. Kahn, *Adv. Inorg. Chem.* **1995**, 43, 179; b) W. Linert, M. Verdaguer, *Molecular Magnets. Recent Highlights*, Springer, Heidelberg, **2003**.
- [9] a) E. Pardo, R. Ruiz-García, F. Lloret, J. Faus, M. Julve, Y. Journaux, F. S. Delgado, C. Ruiz-Pérez, *Adv. Mater.* **2004**, 16, 1597; b) E. Pardo, R. Ruiz-García, F. Lloret, J. Faus, M. Julve, Y. Journaux, M. A. Novak, F. S. Delgado, C. Ruiz-Pérez, *Chem. Eur. J.* **2007**, 13, 2054.
- [10] a) I. Fernández, R. Ruiz, J. Faus, M. Julve, F. Lloret, J. Cano, X. Ottenwaelder, Y. Journaux, M. C. Muñoz, *Angew. Chem.* **2001**, 113, 3129; *Angew. Chem. Int. Ed.* **2001**, 40, 3039; b) E. Pardo, K. Bernot, M. Julve, F. Lloret, J. Cano, R. Ruiz-García, F. S. Delgado, C. Ruiz-Pérez, X. Ottenwaelder, Y. Journaux, *Inorg. Chem.* **2004**, 43, 2768; c) E. Pardo, R. Ruiz-García, F. Lloret, M. Julve, J. Cano, J. Pasán, C. Ruiz-Pérez, Y. Filali, L. M. Chamoreau, Y. Journaux, *Inorg. Chem.* **2007**, 46, 4504; d) C. L. M. Pereira, E. Pedroso, H. O. Stumpf, M. A. Novak, L. Ricard, R. Ruiz-García, E. Rivière, Y. Journaux, *Angew. Chem.* **2004**, 116, 974; *Angew. Chem. Int. Ed.* **2004**, 43, 956.
- [11] a) E. Pardo, K. Bernot, M. Julve, F. Lloret, J. Cano, R. Ruiz-García, J. Pasán, C. Ruiz-Pérez, X. Ottenwaelder, Y. Journaux, *Chem. Commun.* **2004**, 920; b) E. Pardo, I. Morales-Osorio, M. Julve, F. Lloret, J. Cano, R. Ruiz-García, J. Pasán, C. Ruiz-Pérez, X. Ottenwaelder, Y. Journaux, *Inorg. Chem.* **2004**, 43, 7594.
- [12] X. Ottenwaelder, J. Cano, Y. Journaux, E. Rivière, C. Brennan, M. Nierlich, R. Ruiz-García, *Angew. Chem.* **2004**, 116, 868; *Angew. Chem. Int. Ed.* **2004**, 43, 850.
- [13] a) M. Albrecht, *Chem. Soc. Rev.* **1998**, 27, 281; b) C. A. Schalley, A. Lützen, M. Albrecht, *Chem. Eur. J.* **2004**, 10, 1072; c) M. Albrecht, I. Janser, R. Fröhlich, *Chem. Commun.* **2005**, 157.
- [14] a) G. De Munno, M. Julve, F. Lloret, J. Faus, A. Caneschi, *J. Chem. Soc. Dalton Trans.* **1994**, 1175; b) S. Dominguez, A. Mederos, P. Gili, A. Rancel, A. E. Rivero, F. Brito, F. Lloret, X. Solans, C. Ruiz-Pérez, M. L. Rodríguez, *Inorg. Chim. Acta* **1997**, 255, 367; c) J. M. Herrera, A. Bleuzen, Y. Dromzée, M. Julve, F. Lloret, M. Verdaguer, *Inorg. Chem.* **2003**, 42, 7052; d) A. Rodríguez, H. Sakiyama, N. Masciocchi, S. Galli, N. Galez, F. Lloret, E. Colacio, *Inorg. Chem.* **2005**, 44, 8399; e) D. Maspoch, N. Domingo, D. Ruiz-Molina, K. Wurst, J. M. Hernández, G. Vaughan, C. Rovira, F. Lloret, J. Tejada, J. Veciana, *Chem. Commun.* **2005**, 5035.
- [15] a) V. Mishra, F. Lloret, R. Mukherjee, *Inorg. Chim. Acta* **2006**, 359, 4053; b) D. Maspoch, N. Domingo, D. Ruiz-Molina, K. Wurst, J. M. Hernández, F. Lloret, J. Tejada, C. Rovira, J. Veciana, *Inorg. Chem.* **2007**, 46, 1627; c) A. K. Sharma, F. Lloret, R. Mukherjee, *Inorg. Chem.* **2007**, 46, 5128.